Numerical Simulation of Electron Beam Welding of Aluminum Alloys

Pavol Novák, *Milan* Sága, *Milan* Vaško, *Peter* Kopas, and *Marián* Handrik

University of Žilina, Univerzitná 8215/1, 010 26 Žilina, Slovakia

Abstract. The aim of this paper is to investigate the influence of technological parameters of the welding process on the level of the residual stresses, distortions, and phase proportions. The preheating temperature and the eccentricity of the weld path are taken into account. The Visual Weld tool from ESI Group was used for simulation.

1 Introduction

Numerical simulation of the residual stresses, phase proportions, and distortions for welding joints is very important for choosing the right welding parameters to reduce the cost of each new design of the welded joint. The simulation of laser heating [1] with coupled heat transfer and fluid flow in the fusion zone is very complex analysis. In the Visual Weld environment we simulate welding physics only in the solid state. When the temperature exceeds the liquidus temperature, the history of the plastic deformation is cleared and yield modulus is low.
Simulation of laser beam cutting technology [2] is becoming increasingly popular in various industries. Electron beam welding in the Visual Weld environment uses the same type of heat source like laser welding - 3D conical Gaussian heat source model.
Resulting mechanical properties of aluminum alloys welds [3] are veryimportant for their practical use.

2 Theory

For computations, the Sysweld is used. This software is capable to incorporate phase changes and effects of latent heat in welding simulations. Four phases are used in aluminum welding simulation. The phase number one is used for the initial material of welded parts. It is work-hardened material. The second phase is not yet existing filler material which is initially a very weak material used to simulate the weld bead. It is transformed into other phases according to the CCT diagram which is included in the material data. The third phase is molten material. The fourth phase is the weak recrystallized material. The phase transformations are based on Leblond's model

$$\frac{dP}{dt} = \frac{P_{eq} - P}{\tau}, \qquad (1)$$

where P is the phase proportion, t is time, P_{eq} is the equilibrium value of the phase proportion, τ is the time delay.

3 Numerical example

T joint of two plates made from 5000 series AL alloy is investigated to influence of preheating temperature and eccentricity of the weld path relative to symmetry plane to residual stresses, phase proportions, and distortions. Fig. 1 and Fig. 2 show the clamping conditions of the T joint during the welding process. During the first 200 seconds the thicker plate is fastened with clamps on both ends (Fig. 1) then it is unclamped and statically determinate during the cooling phase (Fig. 2).
The FE mesh used for simulation is shown in Fig. 3 along with dimensions of the welded parts. The mesh consists of 302 684 elements and 278 886 nodes. The weld pool and heat affected zone are meshed by fine brick elements to capture the stress and the temperature gradients as well as phase proportions changes. The mesh is coarsened in other zones to maintain computational efficiency.
At the beginning of the simulation, all plates consist of 100% of phase 1. Phase 1 is work-hardened 5000 series AL alloy which chemical composition is shown in Tab. 1. Initially, the plates are stitched together by spot welds at the beginning, middle, and end of the length of the plates.

Table 1. Chemical composition of AL alloy.

Chemical composition	Percentage (%)
Si	0.25
Fe	0.4
Cu	0.1
Mn	0.5-1.0
Mg	2.4-3.0
Cr	0.05-0.2
Zn	0.25
Ti	0.2

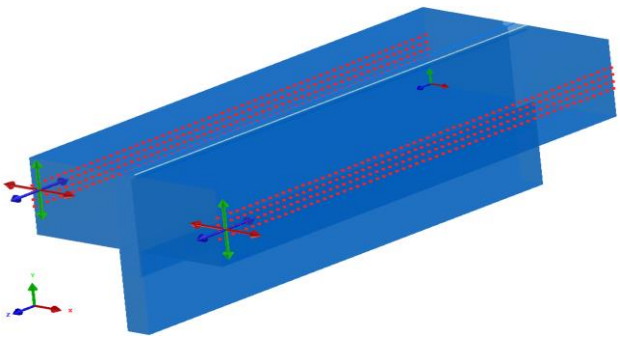

Fig. 1. Clamping conditions for time interval 0-200 sec.

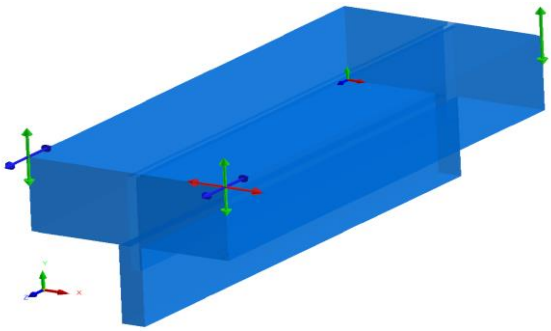

Fig. 2. Clamping conditions (statically determinate) for time interval 200-7200 sec.

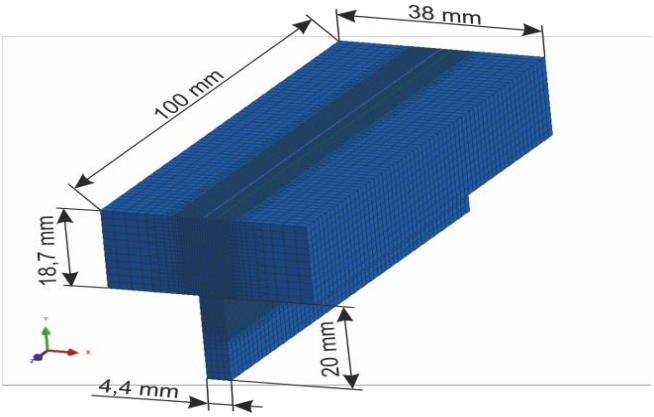

Fig. 3. T joint - FE mesh and dimensions of the welded parts.

4 Results

4.1 Influence of the eccentricity of the weld path

Fig. 4 shows that the eccentricity has no influence on the maximal and minimal displacements of the welded unclamped structure. The differences are in thousandths of a millimeter.

The eccentricity of the weld path have influence on the residual stresses of the unclamped structure (Fig. 5). The von Mises stress is slightly higher at the eccentricity 0.2 mm, but much higher at the eccentricity 0.3 mm. The maximal value of the first principal stress $S_1$with the eccentricity rises only very slightly. The algebraic minimal value of the third principal stress S_3isn't straightforward with the eccentricity of the weld path. Itgoes down with the eccentricity 0.2 mm, but rises with the eccentricity 0.3 mm.

4.2 Influence of the preheating temperature

Fig. 6 shows that the preheating temperature has some influence on the maximal and minimal displacements of the welded unclamped structure. The minimal value of the displacement $U_X$is almost constant. All other values are algebraically decreasing with the preheating temperature. The maximal value of the total displacement decreases very slowly

with increasing preheating temperature. The most significant is the dependence of the minimal value of the displacement $U_Z$on the preheating temperature.
The von Mises, the first principal and third principal stresses are decreasing with rises of preheating temperature. The maximal rate of decreasing of the stresses is achieved for preheating temperature 100 ^{O}C.

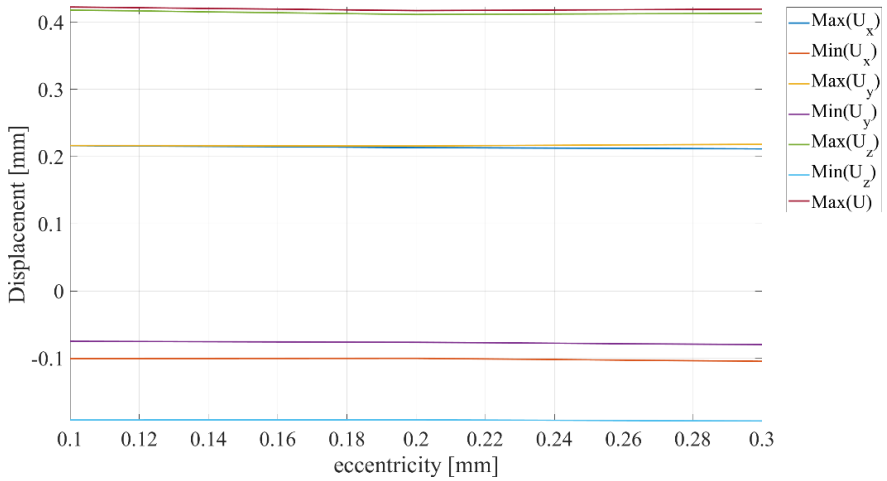

Fig. 4. Maximal and minimal displacements vs. eccentricity of weld joint path.

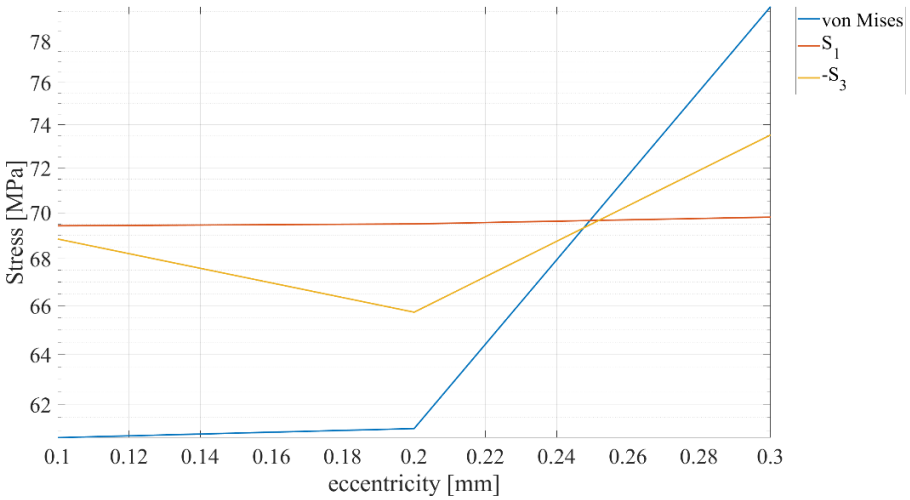

Fig. 5. Von Mises, first principal and minus third principal stresses as function of eccentricity of weld joint path.

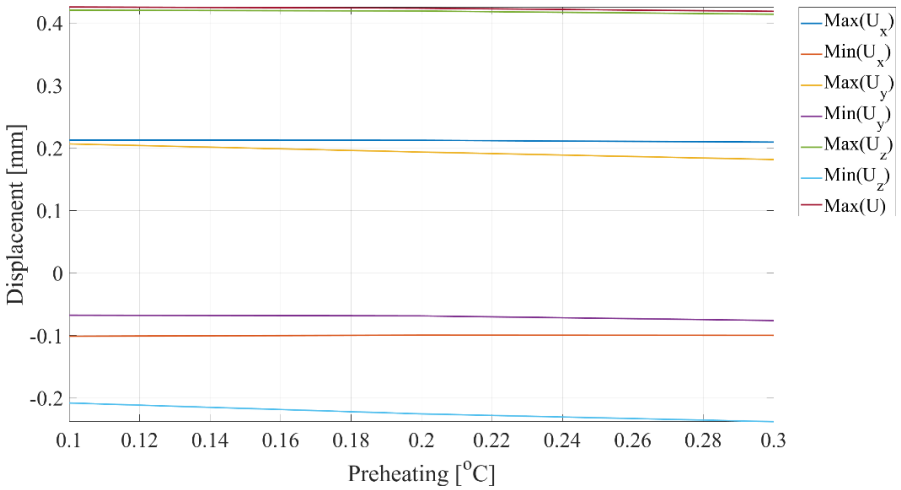

Fig. 6. Maximal and minimal displacements as functions of preheating temperature.

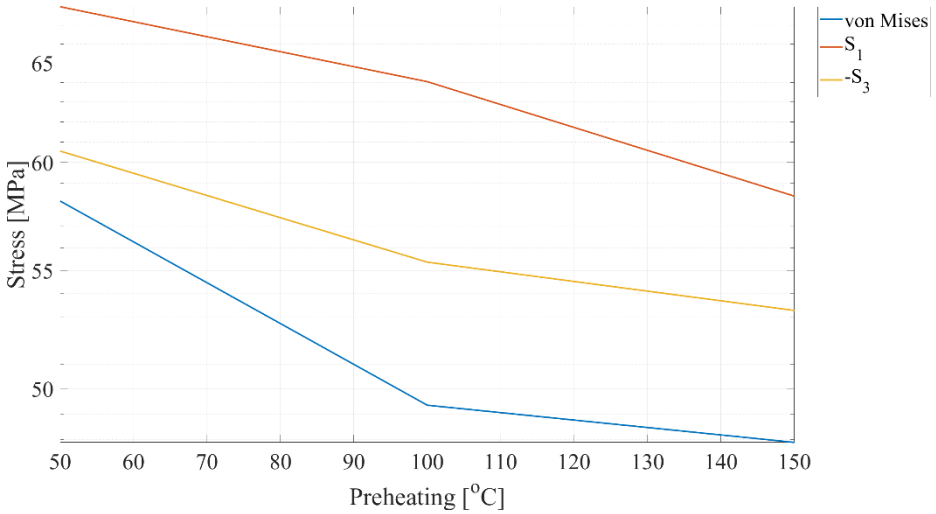

Fig. 7. Von Mises, first principal and minus third principal stresses as function of preheating temperature.

Acknowledgement

The research was supported by Scientific Grant Agency of Ministry of Education, Science and Sport of Slovak Republic in connection with the implementation of the Research of Intelligent Systems and Processes project using the principles of Industry 4.0 with a focus on connecting difficult-to-connect materials with highly concentrated energy sources - laser and electron beam,MŠSR 1227/2018.

References

1. M. Kubiak Prediction of microstructure composition in steel plate heated using high power Yb:YAG laser radiation. In: Malujda, I; Dudziak, M; Krawiec, P. (eds.) MMS 2018, MATEC Web of Conferences, vol. 254, pp. 1–13. MATEC (2019).
2. Z. Saternus, W. Piekarska, M. Kubiak, T. Domanski, D. Goszczynska-Kroliszewska: Numerical modeling of cutting process of steel sheets using a laser beam. In: Malujda, I; Dudziak, M; Krawiec, P. (eds.) MMS 2018, MATEC Web of Conferences, 254, 22-28 (2019).
3. P. Kopas, M. Blatnický, M. Sága, M. Vaško Identification of mechanical properties of weld joints of AlMgSi07.F25 aluminium alloy. Metalurgija 56, 1-2, 99-102 (2017).